Bulgarian Chemical Communications, Volume 50 Special Issue D (pp. 39 – 47) 2018

A Comprehensive Approach to Improve Performance and Stability of State-of-the-Art Air Electrodes for Intermediate Temperature Reversible Cells: An Impedance Spectroscopy Analysis

M. P. Carpanese[1,2 *], D. Clematis[1], M. Viviani[2], S. Presto[2], G. Cerisola[1], M. Panizza[1], M. Delucchi[1], A. Barbucci[1,2]

[1]*Department of Civil, Chemical and Environmental Engineering (DICCA), University of Genova, Via all'Opera Pia 15, 16145 Genova, Italy*

[2]*Institute of Condensed Matter Chemistry and Energy Technologies (ICMATE), National Council of Research (CNR), c/o DICCA-UNIGE, Via all'Opera Pia 15, 16145 Genova, Italy*

Received May 15, 2018 Revised July 12, 2018

Solid oxide fuel cells (SOFC) are devices for the transformation of chemical energy in electrical energy. SOFC appear very promising for their very high efficiency, in addition to the capability to work in reverse mode, which makes them suitable for integration in production units powered with renewables.

Research efforts are currently addressed to find chemically and structurally stable materials, in order to improve performance stability during long-term operation.

In this work, we examine different approaches for improving stability of two state-of-the-art perovskite materials, $La_{0.6}Sr_{0.4}Co_{0.2}Fe_{0.8}O_{3-\delta}$ (LSCF) and $Ba_{0.5}Sr_{0.5}Co_{0.8}Fe_{0.2}O_{3-\delta}$ (BSCF), very promising as air electrodes. Two different systems are considered: (i) LSCF and BSCF porous electrodes impregnated by a nano-sized $La_{0.8}Sr_{0.2}MnO_{3-\delta}$ layer and (ii) LSCF-BSCF composites with the two phases in different volume proportions.

The study considers the results obtained by electrochemical impedance spectroscopy investigation, observing the polarisation resistance (R_p) of each system to evaluate performance in typical SOFC operating conditions. Furthermore, the behaviour of polarisation resistance under the effect of a net current load (cathodic) circulating for hundreds of hours is examined, as parameter to evaluate long-term performance stability.

Key words: LSCF, BSCF, LSM, stability, degradation, overpotential

INTRODUCTION

Among the existing devices devoted to energy production and storage, which could play an important role in the transition toward a sustainable energy scenario, high temperature solid oxide fuel and electrolysis cells (SOFC/SOEC) appear particularly promising.

Cheap catalysts can be used for electrode reactions and high temperature of operation allows obtaining high reaction rates and optimizing thermodynamic efficiencies; furthermore, flexibility of fuels [1-4] and reversible operation [5-11] are feasible, maintaining similar configuration and efficiency. New configurations, exploiting properties of a mixed anionic and protonic conductor used as central membrane [12,13], or taking advantages of a symmetrical configuration in an electrolyte supported cell [14] appear to be useful as reversible solid oxide cells.

Over the past few years, several materials have been investigated as anode materials for SOFC application [15]. Nowadays, Ni-YSZ based anode is widely used for SOFC, although facing long-term instability issues and suffering from carbon and sulfur poisoning and agglomeration of nickel particles at elevated temperature [16,17].

The Perovskite-based materials, such as $La_{0.8}Sr_{0.2}MnO_{3-\delta}$ (LSM), $La_{0.6}Sr_{0.4}Co_{0.2}Fe_{0.8}O_{3-\delta}$ (LSCF) and $Ba_{0.5}Sr_{0.5}Co_{0.8}Fe_{0.2}O_{3-\delta}$ (BSCF) perovskites have been extensively investigated as electrode materials in SOFC/SOEC devices over the last decade, since they can be used efficiently as air-side electrode [18-21]. Anyway, to make this technology affordable in order to gain market penetration, long-term operation without serious degradation must be achieved [22,23].

It has been widely proven that LSM is a stable material and, despite its intrinsically high ion migration energy [24], its oxygen ion diffusion can be strongly increased under reduction conditions, resulting in improvement of its activity [25]. On the other side, LSCF and BSCF, with their high oxygen ion surface exchange and transfer properties, show issues related to chemical and structural instability,

To whom all correspondence should be sent:
E-mail: carpanese@unige.it

which causes degradation during operation time [26-29]. Among the several causes of LSCF degradation, cations interdiffusion between interfaces have been reported as the most harmful, with consequent atoms depletion and phase separation [30].

Concerning BSCF, the same structural properties, which make it so active for oxygen reduction activity, also lead to lattice instability, which is a serious disadvantage for BSCF being considered as a reliable material at SOFC operating conditions.

Many different approaches have been applied in order to stabilise LSCF-based materials, and infiltration/impregnation is one of the most effective [31,32]. LSM has been frequently used as infiltrated continuous or discrete phase, improving in each case performances and stability [33,34].

Also the combination of different materials, based on producing a component that is superior to both of the components separately (generally a composite), has been widely used as an approach to improve properties. In SOFC case, whether it is an electrode [35-38] or an electrolyte [39,40], different conductive phases (ionic and/or electronic) are combined to produce a synergy result or to mitigate some original detrimental effect. Considering the "physiological" inclination of LSCF and BSCF to undergo a cation interdiffusion [22] under prolonged thermal effect or working time, the idea of the authors was to combine these materials to obtain a mutual chemical stabilisation, besides an optimisation of conduction transfer properties [41].

In any case, it is of primary importance to simulate real conditions of operation by the evaluation of the cathode redox behaviour under application of DC (direct current) overpotentials (η), which can drive oxygen incorporation (or release). To this purpose, electrochemical impedance spectroscopy (EIS) is a powerful fundamental technique adapted to the study of SOFC/SOEC systems, since it can be used as *in-situ* tool to characterise the performance of electrodes coupling the effect of a current load.

In this paper, a comprehensive experimental study was performed on the combination of LSM, LSCF and BSCF perovskites, with the purpose of investigating performance and long-term stability of these systems in SOFC working conditions. Two different types of air electrode were considered: *i)* LSCF- and BSCF-based, infiltrated by an LSM-discrete layer and *ii)* mixture of LSCF and BSCF, to obtain cathodes with different compositions of the two phases. The study was carried out mainly through impedance spectroscopy at open circuit (OCV) and under applied overpotential (η), to simulate real conditions of operations.

EXPERIMENTAL

Electrolyte substrates were fabricated from $Ce_{0.8}Sm_{0.2}O_{2-\delta}$ powders (SDC20-HP, Fuel Cell Materials) by cold pressing at 60 MPa, followed by one-step sintering at 1773 K for 5 hours in air. The resulting electrolyte disks had a diameter of 25 mm and a thickness of 1.2 mm. Infiltration procedure was applied on LSCF and BSCF electrodes, which were synthesized through a solution combustion synthesis method based on a mixed-fuel approach. The methodology for synthesis is reported elsewhere [42]. The LSM infiltrated layer was prepared as follows. A 2 M (mol l^{-1}) aqueous solution of $La_{0.8}Sr_{0.2}MnO_{3-\delta}$ precursors was prepared by dissolving proper amounts of $La(NO_3)_3 \cdot 6H_2O$ (99%), $Sr(NO_3)_2$ (>99%), and $Mn(NO_3)_2 \cdot 4H_2O$ (98%) (Sigma Aldrich) in distilled water, at room temperature. In order to better control phase formation and morphology, glycine (Sigma Aldrich) as chelating agent (volume ratio of glycine to LSM ~ 2.5:1) and polyvinyl pyrrolidone (PVP, Sigma Aldrich) as surfactant (0.05 wt% of LSM amount) were added to the metal nitrate solution. The solution was then heated to 473 K and stirred until a gel was obtained which was appropriate for cathode infiltration. A detailed description for infiltration is reported in a previous work [43]

Mixture of $Ba_{0.5}Sr_{0.5}Co_{0.8}Fe_{0.2}O_{3-\delta}$ (BSCF, Treibacher Industrie AG) and $La_{0.6}Sr_{0.4}Co_{0.2}Fe_{0.8}O_{3-\delta}$ (LSCF, FuelCellMaterials) commercial powders with three different volume ratios 50-50 v/v% (BL50), 70-30 v/v% (BL70) and 30-70 v/v% (BL30), were prepared using ball milling in distilled water for 20 h at room temperature. The procedure for the fabrication of the LSCF-BSCF composite electrodes is described in detail in a previous paper [39].

LSCF, BSCF and composite electrodes were deposited by slurry coating after mixing the powder in a mortar with alpha-therpineol (techn. 90%, Sigma Aldrich), to obtain suitable ink.

All the cells were prepared in three-electrode configuration and symmetry between working electrode (WE) and counter electrode (CE) was achieved by using a mask system. The reference electrode (RE) was placed on the WE side at a distance of 3 times the electrolyte thickness, as suggested in the literature to avoid polarization problems during impedance measurements [44,45]. All the cathodes were sintered at 1100 °C for 2 hours, obtaining after sintering a geometric area of 0.28 cm^2. The electrochemical impedance

spectroscopy (EIS) investigation was carried out with a potentiostat coupled to a frequency response analyzer (Autolab PGSTAT302N). Impedance measurements were performed both at open circuit voltage (OCV) and at applied cathodic overpotential (from −0.1 up to −0.3 V), applying a perturbation of 10 mV and between 0.1 Hz and 100 kHz of frequency range. Before performing the systematic electrochemical cell characterization, measurements of the cell rig inductance as well as a check on system linearity were carried out to obtain high quality EIS data [46]. Ageing tests were performed by applying a cathodic direct current (dc) of 200 mA cm^{-2} and checking the system evolution by impedance measurements at OCV, after interruption of the dc load at different times.

To observe cathode degradation, the polarization resistance (R_p) was evaluated as the difference between the low and high frequency intercepts with the real axis in the EIS Nyquist plots. Electrochemical impedance spectroscopy (EIS) measurements were carried out in a lab-constructed test station [47].

RESULTS AND DISCUSSION

Electrode performances – results of LSM infiltration and phase mixing

In Fig. 1 SEM images of LSM-LSCF and LSM-BSCF infiltrated electrodes are reported. The nanosized LSM layer is clearly visible on the electrode backbones. The electrochemical activity of LSCF and BSCF reference and infiltrated cathodes was evaluated with impedance measurements, whose results are reported in Fig. 1.

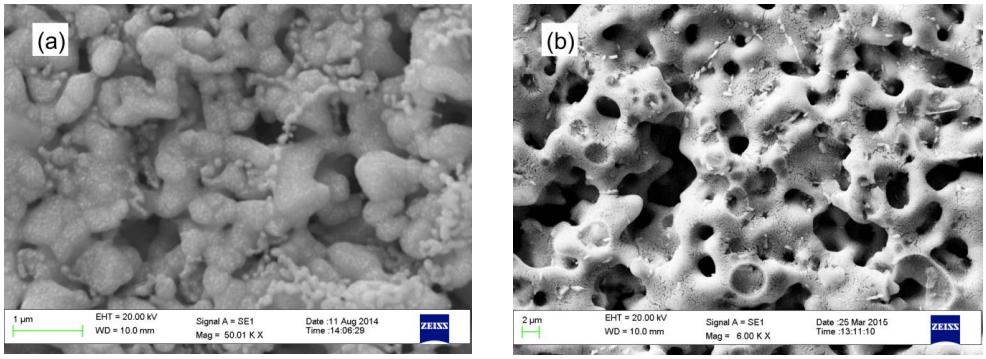

Fig. 1. SEM images of the top surfaces of the (a) LSM-LSCF and (b) LSM-BSCF infiltrated electrodes. The nano-sized LSM layer is apparent as the distributed phase on the porous backbones.

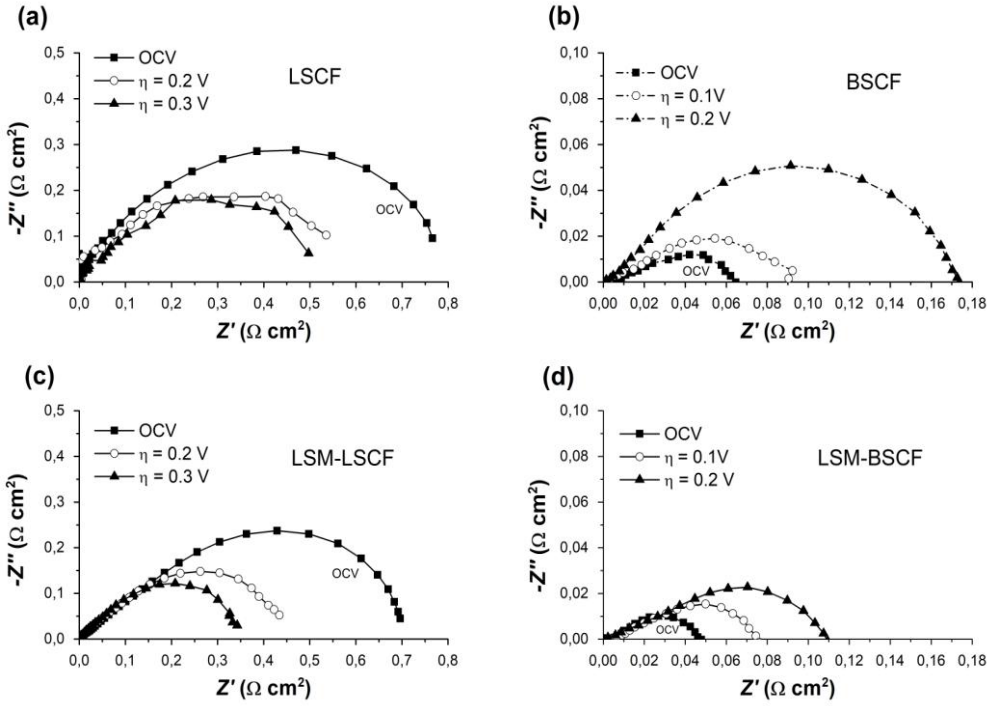

Fig. 2. Impedance spectra of the reference and LSM-impregnated LSCF cathodes ((a) and(c), respectively), and of the reference and LSM-impregnated BSCF cathodes ((b) and (d), respectively), at OCV and different overpotentials (η). Measurements conditions: 700 °C, 21% O_2 partial pressure; η: −0.1 V to −0.3 V (−0.2 V for BSCF).

The impregnation, applied with the purpose of stabilizing the initial cathode performances over time, produced, as expected, an improvement in the cathodic electrocatalytic activity, both in LSCF-based (Figs. 2a and 2c) and in BSCF-based (Figs. 2b and 2d) electrodes.It is worth highlighting that BSCF polarization resistance is one order of magnitude lower than in LSCF. Although LSCF and BSCF are mixed ionic-electronic conductors with substantial oxygen ions and electrons transport properties, the discrete and nano-sized LSM surface coverage introduced extra specific surface area, available for the oxygen exchange reaction at the cathode/gas interface.

This resulted in further improvement to the cathode electro-catalytic activity, both at OCV and when a net cathodic current flowed across the sample (applied η). At OCV, LSCF polarization resistance R_p decreased from about 0.78 Ω cm^2 at 700 °C, to 0.69 Ω cm^2 for the LSM-impregnated (see Figs. 2a and 2c). The improvement of BSCF in terms of R_p was from 0.066 Ω cm^2 to 0.046 Ω cm^2 (see Figs. 2b and 2d).

The results observed against the cathodic overpotential (η) appeared very interesting, since the behavior of BSCF and LSCF was contrasting. In Figs. 2a and 2c the Nyquist plots of LSCF and LSM-impregnated LSCF cathodes at OCV, η=−0.1V, η=−0.2Vand η =−0.3 V are reported. Cathodic polarization (η) has a beneficial effect, in terms of the reduction reaction kinetic, in both reference and impregnated LSCF performance, as pointed out by the decreasing trend of the polarization resistance. On the other hand, the trend of impedance spectra for the reference and impregnated BSCF electrodes, at OCV, η =−0.1 V and at η =−0.2 V conditions, shows that R_p increases with η (Figs. 2b and 2d).

It has been proposed for LSM and LSCF that, when electrons are injected by the applied overpotential, oxygen vacancies are formed to maintain charge neutrality [48,49]. This increase in vacancy concentration causes in LSM a change of kinetic regime, from a "surface" path to a "bulk" path, when a cathodic overpotential is applied higher than 0.2 V [19,20,50]. A similar improvement in the capability to incorporate and transfer oxygen ions takes place in LSCF. This clearly produces an improvement in oxygen surface activity and, in our study, this mechanism likely accounts for the impedance arch decrease displayed in Fig. 1 for LSCF-based cathodes: the synergic effect of LSM and LSCF results in the progressive decrease of the polarization resistance, as the potential applied increases. This improvement in activity is highlighted for LSM-LSCF (Fig. 2c), compared to pristine LSCF (Fig. 2a), both at OCV and under η.

Conversely, according to our results, in BSCF-based cathodes the situation appears quite different, since R_p increases as overpotential increases (Figs. 2b and d). Of course, there is a different way in which the injection of electrons influences the vacancies concentration, surmising that under the applied overpotential the formation of new vacancies is likely suppressed, resulting in the progressive decrease of oxygen activity [51,52]. It can be surmised that BSCF already has its largest concentration of oxygen vacancies before polarization, explaining the value observed of R_p lower for OCV conditions than for polarization, being this evident both for pristine and for LSM-BSCF electrodes (Fig. 2b and 2d, respectively). Similar phenomenon has been observed for other materials, which also have a large concentration of oxygen vacancies at room temperature [53,54]. If this is the case, the slower increase in R_p (Figs. 2b and d) observed for the infiltrated BSCF electrode (with respect to the pure one), has to be explained by the positive contribution of LSM, whose vacancy concentration increases and remains active, although not being able to compensate the opposite behavior of the scaffold material. Nevertheless, the results presented here show that BSCF-based electrodes decrease their activity under the reducing conditions caused by the increased cathodic overpotential.

Considering the electrodes made of LSCF and BSCF mixture, excellent results in terms of electrochemical performances were obtained, extracted in three-electrode configuration. In Fig. 3a impedance spectra of the three compositions (BL70, BL50 and BL 30) are reported at 650 °C, as compared to the those of the pristine LSCF and BSCF electrodes: considering the polarization resistance, all the composite cathodes displayed very promising performances, as compared to the literature, particularly to BSCF-based electrodes, which still remain the reference among state-of-the-art perovskite-based cathodes for SOFCs [55,56]. It is worth highlighting the excellent activity observed for BL70 sample and also for BL50 at this temperature: 0.021 and 0.027 Ω cm^2, respectively. Also BL30 sample showed improved performance of 0.045 Ω cm^2, if compared to the pure starting materials.

In Fig 3b the inverse of the global polarization resistance is reported ($1/R_p$), as function of temperature. In each case, an Arrhenius-type behavior was obtained and the corresponding activation energy was calculated. Despite its higher resistivity, BL30 shows the lower activation energy

value, 0.96 eV, indicating this composition as very suitable for low temperature of operation. BL70 shows an activation energy equal to 1.17 eV, very closed to that of pure BSCF (1.17 eV) and lower than pure LSCF (1.52 eV). The values obtained are in agreement with the literature (LSCF 1.45 eV [57] and BSCF 1.20 eV [58,59]).

Performance stability under current load

In order to evaluate the influence of the impregnation on cell performance stability, all the systems were tested over time at 700 °C under a DC current load of 200 mA cm^{-2} at 21% O_2 partial pressure. During the test, the current was periodically interrupted for the time necessary to perform OCV EIS measurements, in order to follow up the degradation of the electrode activity. The results obtained for the infiltrated system are reported in Figs. 4a and 4b. Degradation of electrode performance in the first operating hours is reported as key factor, because the analysis of performance losses in the first 100-300 working hours is often considered a good indication to evaluate electrode long-term stability [60-63].

Consequently, an ageing time of 200 hours was chosen to monitor the evolution of the LSCF system (Fig. 4a). For the BSCF-based system the ageing time was prolonged until 720 h of current load (Fig. 4b). In the case of the pristine LSCF cathode, a remarkable R_p increase (from 0.8 Ω cm^2 to 1.03 Ω cm^2) is visible already in the first 72 hours of working time, showing a 29% performance degradation, in accordance with that reported in literature [59,60,61].

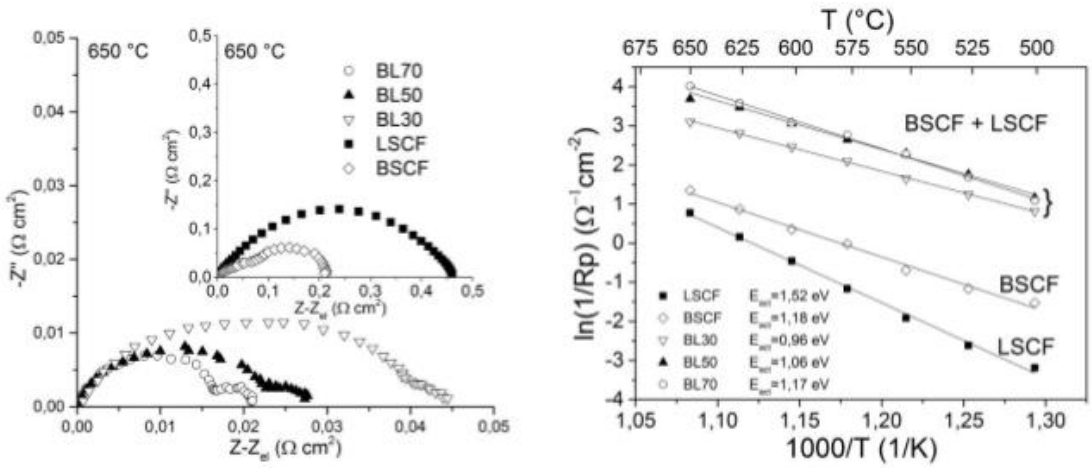

Fig. 3. (a) Impedance spectra at 650 °C and OCV for BL30, BL50, BL70. The inset shows impedance spectra for pure BSCF and LSCF. (b) Arrhenius plot for the five cathodes and calculated activation energy: BL30 (0.95 eV), BL50 (1.06 eV), BL70 (1.17 eV), BSCF (1.18 eV) and LSCF (1.52 eV).

Conversely, the polarization resistance related to the LSM-infiltrated LSCF electrode decreases over time from 0.7 Ω cm^2 to 0.515 Ω cm^2 (26% decrease) in 220 hours (see Fig. 4a), confirming a positive effect of the LSM infiltration on the long-term stability of the LSCF electrode. A meaningful effect due to the LSM impregnation is also observed on the BSCF electrodes (Fig. 4b).Although the LSM coating cannot prevent the increase in polarization resistance over time, it contributes to hindering BSCF degradation. According to other author [64] a possible beneficial effect on BSCF (which appears also in LSCF-based cathodes) could be related to a desirable cation inter-diffusion between the LSM and backbone, enable in inhibit structural modifications, albeit without blocking them altogether.

Considering an ageing time of 200 hours, for the LSM-impregnated BSCF electrodes R_p increases from 0.046 Ω cm^2 up to 0.08 Ω cm^2, with 74% of degradation, while R_p for the reference BSCF cathode increases from 0.081 Ω cm^2 to 0.16 Ω cm^2, with 98% of degradation. A comparable degradation is reached in the LSM-infiltrated BSCF electrode after 750 hours of working time (Fig. 4b).

Looking at the composite system, similar ageing tests were carried out, at the working temperature of 650 °C. All the electrodes showed a remarkable R_p increase in the first 24 h and each sample showed a different degradation rate. Anyway, after 75 hours of applied current load, in any case a slowdown on the R_p increase was observed (Fig. 5).

In particular, for BL70 sample, which is the most active electrode, three different intervals were identified, characterized by a different degradation rate: 0 - 24 h, 24-75 h and 75-200 h. Starting degradation was calculated as 6.67 x 10^{-4} Ω cm^2 h^{-1}, being this value in agreement with those extrapolated for BSCF and LSCF by the authors (~10^{-3} to 10^{-4} Ω cm^2 h^{-1}) and other authors [39,65].

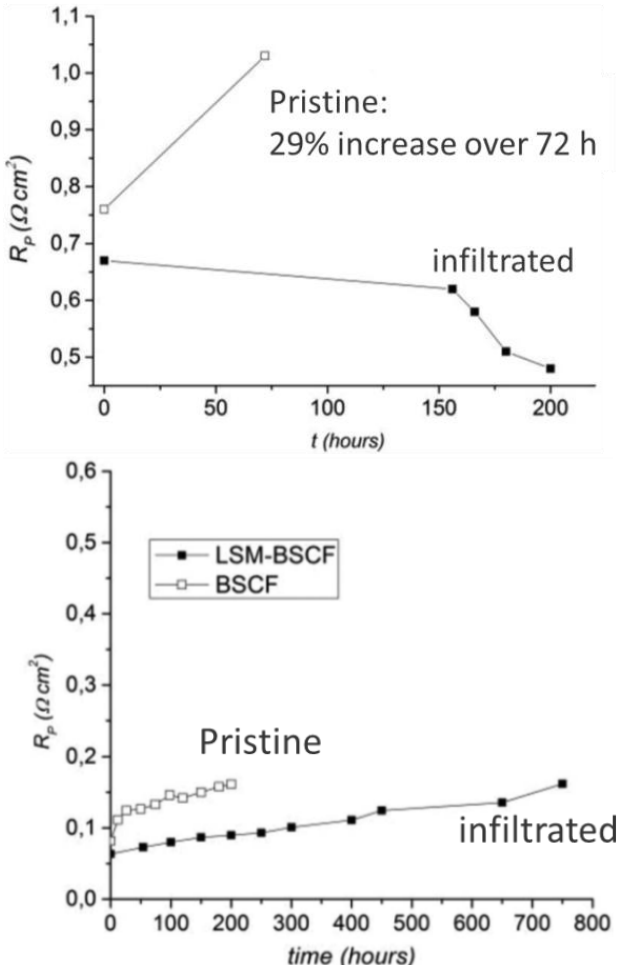

Fig. 4. Trend of the cathode polarization resistance (Rp) over time for (a) reference and LSM-infiltrated LSCF cathode and for (b) reference and LSM-infiltrated BSCF, during the ageing test under cathodic current load of 200 mAcm^{-2}. Conditions: 700 °C, OCV and 21% O_2 partial pressure. The testing duration time was 200 h for LSM-LSCF and 750 h for LSM-BSCF.

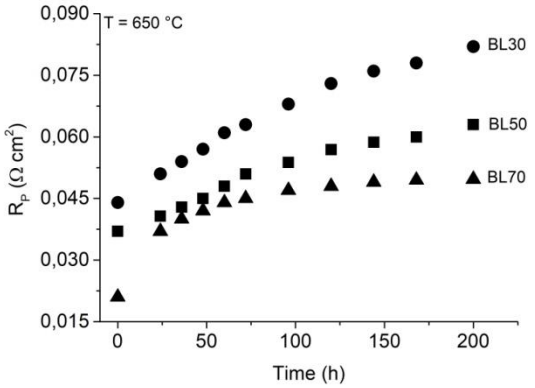

Fig. 5. Degradation rate for BL30, BL50, BL70 electrodes under an applied current load of 200 mA cm^{-2} at 650 °C.

In the final part of the ageing test (75 to 200 h) a trend toward 10^{-5} Ω cm^2 h^{-1} was evaluated, which represents an improvement in terms of stability. It is worth noticing that BL70 degradation rate slowdown had a positive effect on polarization resistance, which reached a noteworthy constant R_p value close to 0.048 Ω cm^2 (@650 °C), lower than those reported in literature by several authors for pure and fresh LSCF and BSCF electrodes [66,67] and comparable to data reported for BLSCF [64].

CONCLUSIONS

A diversified approach was carried out to increase long-term stability of perovskite-based materials, such as LSCF and BSCF. Two different systems were considered: (i) LSCF- and BSCF-porous electrodes, infiltrated by a nano-sized discrete layer of LSM and (ii) mixture of LSCF and BSCF materials to obtain composites with different amount of the two phases. The systems were characterized as cathodes on SDC electrolytes, in SOFC conditions of operation, by electrochemical impedance spectroscopy, in order to evaluate both cathode performance in terms of polarization resistance (R_p, at OCV and under applied cathodic overpotential, η) and long-term stability, by applying a current load of 200 mA cm^{-2} for 200 or 720 h, depending on LSCF or BSCF, respectively.

Very interesting results were found: LSM-impregnation had beneficial effects on the performance of LSCF and BSCF systems. The nano-sized layer on the cathode surface made available new surface area, resulting in improved oxygen surface exchange both at OCV and under applied η. Nevertheless, a contrasting behavior was highlighted for LSCF and BSCF when an increasing η was superimposed: it was apparent that, while LSCF-based electrodes improved their behaviour under reducing conditions, BSCF-based cathodes decreased their activity when a cathodic overpotential was applied.

Looking at the composite LSCF-BSCF electrodes, they revealed an excellent activity towards the oxygen reduction reaction. Particularly, BL70 sample showed an R_p value of 0.021 Ω cm^2 at 650 °C, confirming this composition as very promising to be used as cathode for low temperature SOFCs.

Although the results obtained from the long test under current load confirmed that LSCF and BSCF are intrinsically unstable materials, the two strategies pursued in this work to hinder degradation gave promising results. The polarization resistance of the LSM-LSCF electrodes decreased from 0.7 to 0.51 Ω cm^2 in 220 h at 700 °C, indicating even an improvement in electrocatalytic behavior over time. In the case of LSM-BSCF system, LSM layer could not totally compensate the BSCF degradation, although it

contributed to hinder it remarkably over almost 750 h of ageing test.

Considering the effect of LSCF and BSCF mixing on long-term stability, this appeared strongly correlated to the relative amount of the two phases. It has to be highlighted that the composition BL70, which showed an extremely low R_p value (0.021 Ω cm^2 at 650 °C), was also the one, which degraded more slowly. At the end of ageing time of 200 h, its R_p value was actually enough low to make BL70 composition as suitable for further promising investigation.

REFERENCES

1. A. Jun, Y.-W.Ju, G. Kim, *Faraday Discuss.*, **182**, 519 (2015).
2. A. Buttler, H. Spliethoff, *Renew. Sust. Energ. Rev.*, **82**, 2440 (2018).
3. N. Q. Minh, J. Mizusaki, S. C. Singhal, *ECS Transactions*, **78** (1) 63 (2017).
4. S. Presto, A. Barbucci, M. P. Carpanese, M. Viviani, R. Marazza, J. *Appl. Electrochem.*, **39**, 2257 (2009).
5. M. Viviani, G. Canu, M. P. Carpanese, A. Barbucci, A. Sanson, E. Mercadelli, C. Nicolella, D. Vladikova, Z. Stoynov, A. Chesnaud, A. Thorel, Z. Ilhan, S.-A. Ansar, *Energy Procedia*, **28**, 182 (2012).
6. S. Park, Y. Shao, J. Liu, Y. Wang, *Energy Environ. Sci.*, **5**, 9331 (2012).
7. D. Vladikova, Z. Stoynov, A. Chesnaud, A. Thorel, M. Viviani, A. Barbucci, G. Raikova, P. Carpanese, M. Krapchanska, E. Mladenova, *Int. J. Hydrogen Energy*, **39**, 21561 (2014).
8. C. H. Wendel, Z. Gao, S. A. Barnett, R. J. Braun, *J. Power Sourc*., **283,** 329 (2015).
9. P. Puengjinda, H. Nishino, K. Kakinuma, M. E. Brito, H. Uchida, *J. Electrochem. Soc.*, 164 (9), F889 (2017).
10. M. P. Carpanese, A. Barbucci, G. Canu, M. Viviani, *Solid State Ionics*, **269**, 80 (2015).
11. M. Hauck, S. Herrmann, H. Spliethoff, *Int. J. Hydrog. Energy*, **42** (15), 10329 (2017).
12. Thorel, A. S.; Abreu, J.; Ansar, S.-A.; Barbucci, A.; Brylewski, T.; Chesnaud, A.; Ilhan, Z.; Piccardo, P.; Prazuch, J.; Presto, S.; Przybylski, K.; Soysal, D.; Stoynov, Z.; Viviani, M.; Vladikova D. *Journal of The Electrochemical Society*, **160**(4), F360, (2013).
13. Presto, S.; Barbucci, A.; Viviani, M.; Ilhan, Z.; Ansar, S.-A.; Soysal, D.; Thorel, A. S.; Abreu, J.; Chesnaud, A.; Politova, T.; Przybylski, K.; Prazuch, J.; Brylewski, T.; Zhao, Z.; Vladikova, D.; Stoynov Z., *ECS Transactions*, **25** (2), 773 (2009).
14. Xu, J. ; Zhou, X.; Cheng, J.; Pan, L.; Wu; M.; Dong, X.; Sun, K., *Electrochimica Acta*, **257**, 64 (2017).
15. F. S. Silva, T. M. Souza, *Int. Journal of Hydrogen Energy*, **42** 26020 (2017).
16. Matsuzaki, Y.; Yasuda, I., *Solid State Ionics*, **132**, 261 (2000).
17. Khan, M. S.; Lee, S.-B.; Song, R.-H.; Lee, J.-W.; Lima, T.-H.; Park, S.-J., *Ceramics International*, **42**, 35 (2016).
18. J. Areum, K. Junyoung, S. Jeeyoung, K. Guntae, *ChemElectroChem.*, **3**, 511 (2016).
19. M. P. Carpanese, D. Clematis, A. Bertei, A. Giuliano, A. Sanson, E. Mercadelli, C. Nicolella, A. Barbucci, *Solid state Ionics*, **301**, 106 (2017).
20. A. Bertei, M. P. Carpanese, D. Clematis, A. Barbucci, M. Z. Bazant, C. Nicolella, *Solid State Ionics*, **303**, 181 (2017).
21. D. Heidari, S. Javadpour, S. H. Chan, *Energy Conversion and Management*, **136**, 78 (2017).
22. A. Gondolini, E. Mercadelli, A. Sangiorgi, A. Sanson, *J. Europ. Cer. Soc.*, **37** (3), 1023 (2017).
23. E. Mercadelli, A. Gondolini, P. pinasco, A. Sanson, *Metals Materials Int.*, **23** (1) 184 (2017).
24. M. M. Kuklja, E. A. Kotomin, R. Merkle, Y. A. Mastrikov, J. Maier, *Phys. Chem. Chem. Phys.*, **15**, 5443 (2013).
25. X. J. Chen, K. A. Khor, S. H. Chan, *Solid State Ionics*, **167**, 379 (2014).
26. R. Kiebach, W.-w. Zhang, W. Zhang, M. Chen, K. Norrman, H.-j. Wang, J.R. Bowen, R. Barfod, P. Vang, *J. Power Sources*, **283**, 151 (2015).
27. C. C. Wang, T. Becker, K. Chen, L. Zhao, B. Wei, S. P. Jiang, *Electrochim. Acta*, **139**, 173 (2014).
28. M. M. Kuklja, Y. A. Mastrikov, B. Jansang, E. A. Kotomin, *J. Phys. Chem. C*, **116**, 18605 (2012).
29. H. Gasparyan, J. B. Claridge, M. J. Rosseinsky, *J. Mater. Chem. A*, **3**, 18265 (2015).
30. J. S. Hardy, C. A. Coyle, J. F. Bonnett, J. W. Templeton, N. L. Canfield, D. J. Edwards, S. M. Mahserejian, L. Ge, B. J. Ingram, J. W. Stevenson, *J. Mater. Chem. A*, **6**, 1787 (2018).
31. T. E. Burye and J. D. Nicholas, *J. Power Sources*, **301**, 287 (2016).
32. A. J. Samson, M. Søgaard, P. V. Hendriksen, *Electrochim. Acta*, **229**, 73 (2017).
33. M. E. Lynch, L. Yang, W. Qin, J.-J. Choi, M. Liu, K. Blinn, and M. Liu, *En. Environm. Science*, **4**, 2249 (2011).
34. L. Almar, A. Morata, M. Torrell, M. Gong, T. Andreu, M. Liu, A. Tarancón, *Electrochim. Acta*, **235**, 646 (2017).
35. L. Navarrete, M. Balaguer, V. B. Vert, J. M. Serra, *Fuel Cells*, **17** (1), 100 (2017).
36. N. V. Lyskov, L. M. Kolchina, M. Z. Galin, G. N. Mazo, *Solid State Ionics*, **319**, 156 (2018).
37. A. Barbucci, M. P. Carpanese, M. Viviani, N. Vatistas, C. Nicolella, *J. Appl. Electrochem.*, **39**, 513 (2009).
38. A. Bertei, A. Barbucci, M. P. Carpanese, M. Viviani, C. Nicolella, *Chem. Eng. J.*, **2017-208**, 167 (2012).
39. Y. Yuan, T. Li, H. Nishijima, W. Pan, J. Gong, K. Wang, M. Wang, M. Zhang, X. Zhao, *J. Am. Ceram. Soc.*, **101**, 3130 (2018).
40. I. Khan, P. K. Tiwari, S. Basu, *Ionics*, **24** (1), 211 (2018).
41. A. Giuliano, M. P. Carpanese, M. Panizza, G. Cerisola, D. Clematis, A. Barbucci, *Electrochim. Acta*, **240**, 258 (2017).
42. F. Deganello, L. F. Liotta, G. Macrìı, E. Fabbri, and E. Traversa, *Materials for Renewable and Sustainable Energy*, **2,** 8 (2013).

43. A. Giuliano, M. P. Carpanese, D. Clematis, M. Boaro, A. Pappacena, F. Deganello, L. F. Liotta, A. Barbucci, *J. Electrochem. Soc.*, **164** (10), F3114 (2017).
44. M. Cimenti, V.I. Birss, J.M. Hill, *Fuel Cells*, **7**(5), 377, (2007).
45. J. Winkler, P. V. Hendriksen, N. Bonanos, M. Mogensen, *J. Electrochem. Soc.*,**145** (4), 1184 (1998).
46. G. Raikova, M. P. Carpanese, Z. Stoynov, D. Vladivkova, M. Viviani, A. Barbucci, *Bulg. Chem. Commun.*, **41**, 199 (2009).
47. M. P. Carpanese, M. Panizza, M. Viviani, E. Mercadelli, A. Sanson, A. Barbucci, *J. Appl. Electrochem.*, **45**, 657 (2015).
48. D.N.Müller, M. L.Machala, H.Bluhm, W. C.Chueh, *Nature Commun.*, **6**, 6097 (2015).
49. M. H. R. Lankhorst and J. E. ten Elshof, *J. Solid State Chem.*, **130**, 302 (1997).
50. F. H. van Heuveln, H. J. M. Biuwmeester, F. P. F. van Berkel, *J. Electrochem. Soc.*, **144** (1), 126 (1997).
51. A. S. Harvey, F. J. Litterst, Z. Yang, J. L. M. Rupp, A. Infortuna, and L. J. Gauckler, *Phys. Chem. Chem. Phys.*, **11**, 3090 (2009).
52. V. Bisogni, S. Catalano, R. J. Green, M. Gibert, R. Scherwitzl, Y. Huang, V. N. Strocov, P. Zubko, S. Balandeh, J. M. Triscone, G. Sawatzky, and T. Schmitt, *Nat Commun.*, **7**, 13017 (2016).
53. A. E. Bocquet, A. Fujimori, T. Mizokawa, T. Saitoh, H. Namatame, S. Suga, N. Kimizuka, Y. Takeda, and M. Takano, *Phys. Rev. B*, **45**, 1561 (1992).
54. M. Abbate, G. Zampieri, J. Okamoto, A. Fujimori, S. Kawasaki, and M. Takano, *Phys. Rev. B*, **65**, 165120 (2002).
55. L. Almar, H. Störmer, M. Meffert, J. Szász, F. Wankmüller, D. Gerthsen, E. Ivers-Tiffée, *Appl. En. Mater.*, **1**, 1316 (2018).
56. J. Areum, K. Junyoung, S. Jeeyoung, K. Guntae, *ChemElectroChem.*, **3**, 511 (2016).
57. J. M. Serra, J. Garcia-Fayos, S. Baumann, F. Schulze-Küppers, W. A. Meulenberg, *J. Memb. Sc.*, **447**, 297 (2013).
58. C. Duan, D. Hock, Y. Chen, J. Tong, R. O'Hayre, *Energy Environ. Sci*, **10**, 176 (2017).
59. Z. Shao and S. M. Haile, *Nature*, 431, 170 (2004).
60. J. Kim, S. Choi, A. Jun, H. Y. Jeong, J. Shin, G. Kim, *ChemSusChem*, **7,** 1669 (2014).
61. L.Zhi-Peng, T. Mori, J. A. Graeme, Z. Jin, J. Drennan, *Appl. Mater. Interfaces*, **3**, 2772 (2011).
62. S. P. Simner, M. D. Anderson, M. H. Engelhard, and J. W. Stevenson, *Electroch. Solid-State Lett.*, **9**, A478 (2006).
63. L. dos Santos-Gómez, J. M. Porras-Vázquez, E. R. Losilla, F. Martín, J. R. Ramos-Barrado, and D. Marrero-López, *J. Power Sources*, **347**, 178 (2017).
64. D. Ding, M. Liu, Z. Liu, X. Li, K. Blinn, X. Zhu, and M. Liu, *Adv. En. Mat.*, **3**, 1149 (2013).
65. B. Hirschorn, M. E. Orazem, B. Tribollet, V. Vivier, I. Frateur, M. Musiani, *Electrochim. Acta*, **55**, 6218 (2010).
66. X. Zhang, W. Zhang, L. Zhang, J. Meng, F. Meng, X. Liu, J. Meng, *Electrochim. Acta*, **258**, 1096 (2017).
67. L. Almar, J. Szász, A. Weber, E. Ivers-Tiffée, *J. Electrochem. Soc.*, **164**, F289 (2017)

Комплексен подход за подобряване производителността и стабилността на съвременни въздушни електроди за обратими горивни клетки при междинни температурни: анализ чрез импедансна спектроскопия

М.П. Карпанезе[1,2 *], Д. Клематис[1], М. Вивиани[2], С. Престо[2], Г. Герисола[1], М. Паница[1], М. Делучи[1], А. Барбучи[1,2]

[1]*Катедра по гражданско, химическо и екологично инженерство, Университет в Генуа, Виа але Опера Пиа 15, 16145 Генуа, Италия*

[2] *Институт за конвенционална материя по химия и енергийни технологии, Национален за съвет по научни изследвания (CNR) Виа але Опера Пиа 15, 16145 Генуа, Италия*

Постъпила на 15 юни 2018г..; приета на 26 юли 2018г.

(Резюме)

Твърдо оксидните горивни клетки (ТОГК) са устройства за преобразуване на химическа енергия в електрическа енергия. ТОКГ изглеждат много обещаващи предвид тяхната висока ефективност, в допълнение към способността им да работят в обратим режим, което ги прави подходящи за интегриране в системи, захранвани с възобновяеми енергийни източници.

Понастоящем, с помощта на научни изследвания, се полагат големи усилия да се намерят химически и структурно устойчиви материали, с цел за да се подобрят експлоатационните качества и стабилността на работа при дългосрочна експлоатация.

В този труд ние изследваме различни подходи за подобряване на стабилността на два от най-добрите перовскитни материали понастоящем: $La_{0.6}Sr_{0.4}Co_{0.2}Fe_{0.8}O_{3-\delta}$ (LSCF) и $Ba_{0.5}Sr_{0.5}Co_{0.8}Fe_{0.2}O_{3-\delta}$

(BSCF), много обещаващи като въздушни електроди. Разглеждат се две различни системи: i) LSCF и BSCF пористи електроди, импрегнирани с наноразмерен $La_{0.8}Sr_{0.2}MnO_{3-\delta}$ слой и ii) LSCF-BSCF композити с две фази в различни по обем пропорции. Статията разглежда резултатите, получени с помоща на електрохимична импедансна спектроскопия, като чрез измерване на поляризационното съпротивление (R_p) на всяка система, се определят експлоатационните качества при типични за ТОГК операционни условия. Освен това се изследва поведението на поляризационното съпротивление под действието на общо натоварване на тока (катодно) и циклично в продължение на стотици часове, като параметър за оценка на дългосрочната експлоатационна стабилност.